Supporting Information for

2D nanocrystalline ternary selenides Cu_2MSe_4 (M = Mo/W)

Minyuan M. Li, and Sergei A. Ivanov*

Center for Integrated Nanotechnologies, Los Alamos National Laboratory, PO Box 5800, MS 1315; Albuquerque, NM 87185-1315

Table of content

Figure S1

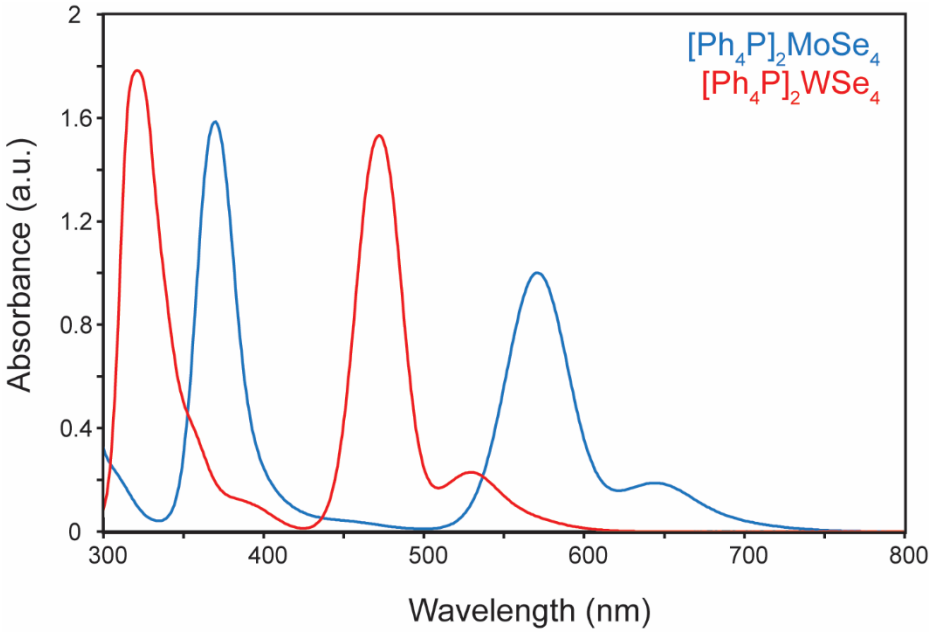

Figure S1. UV-Vis spectra of the tetraphenylphosphonium tetraselenometallate as solutions in DMF.

Figure S2

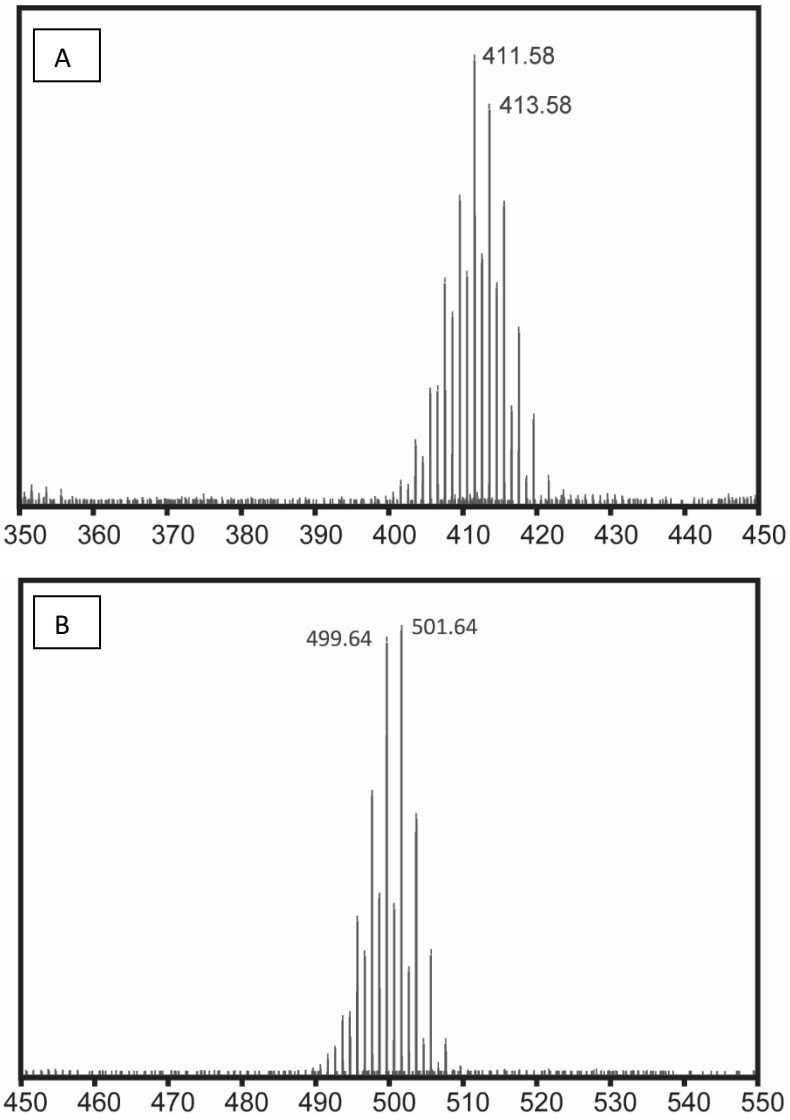

Figure S2. ESI MS spectra of the precursor $[Ph_4P]_2MSe_4$ in negative ion mode. (A) M=Mo, (B) M=W. The patterns correspond to $[MSe_4^{\bullet -}]$ species (MW for $[MoSe_4^{2-}]$ is 411.80 and MW for $[WSe_4^{2-}]$ is 499.68).

.

Figure S3

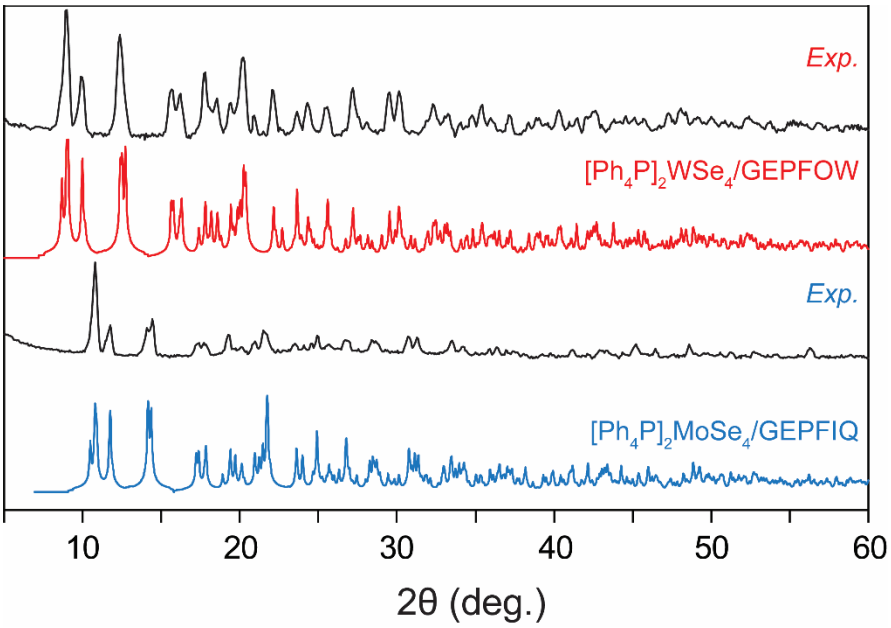

Figure S3. pXRD patterns of $[Ph_4P]_2MSe_4$ materials. Red – M=Mo, Blue – M=W. Reference patterns are shown in colors with their CSD identification codes.

Figure S4

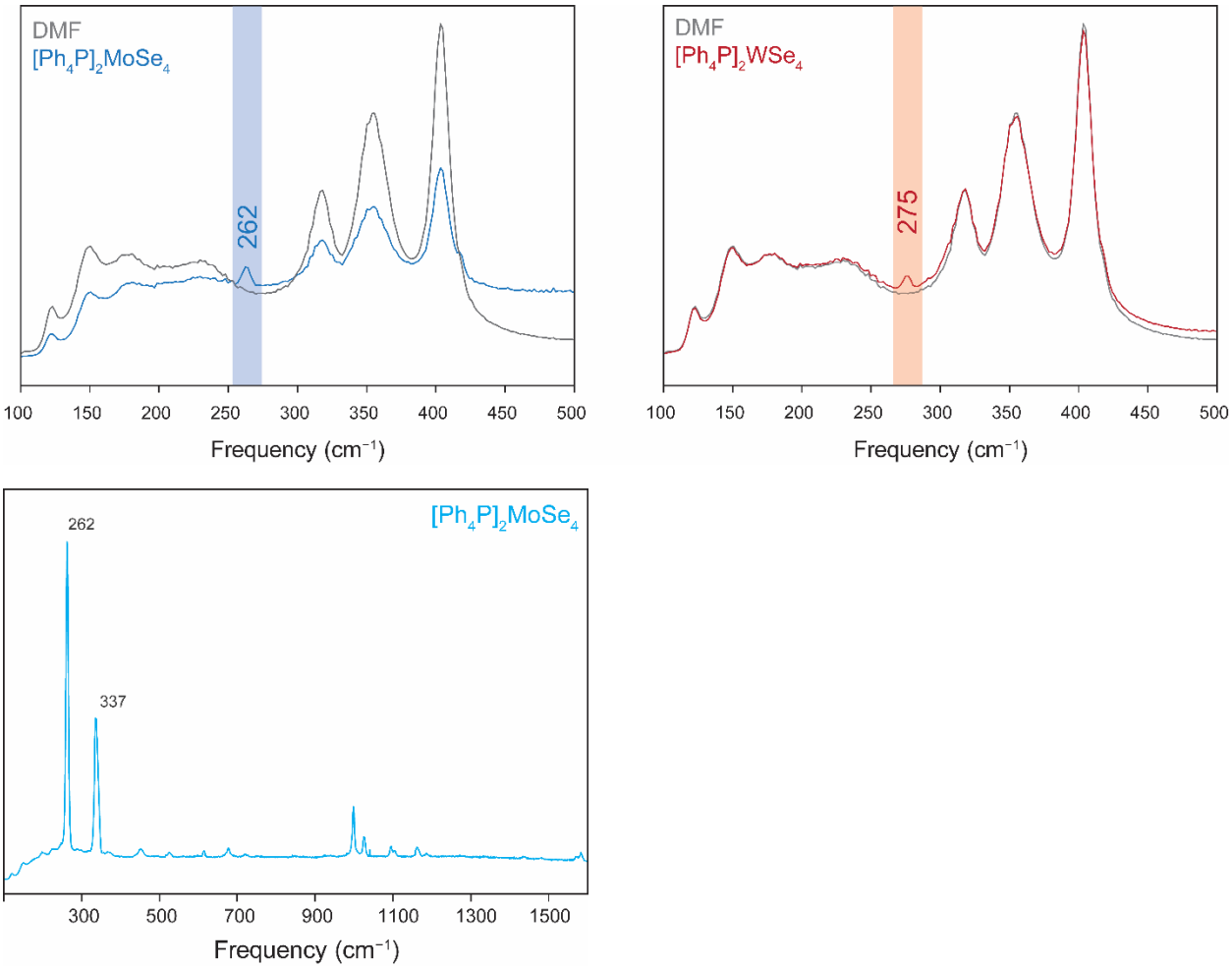

Figure S4. (Top) Raman spectra of DMF solutions of $[Ph_4P]_2MSe_4$ (M = Mo, left panel and M=W, right panel). Spectra of pure DMF are presented in black on both panels. (Bottom) Raman spectrum of $[Ph_4P]_2MoSe_4$ solid.

Figure S5

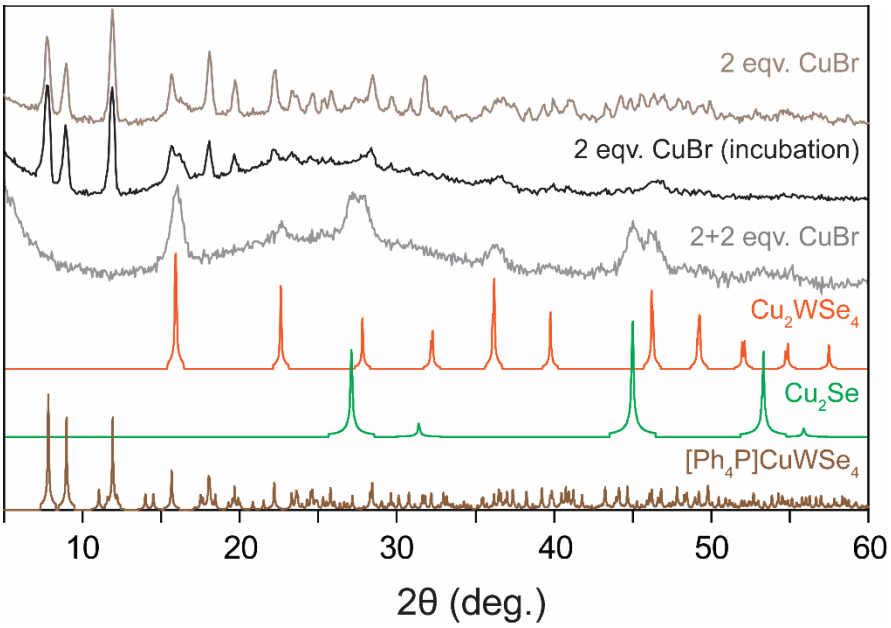

Figure S5. Powder X-ray diffraction pattern of a sample from a 2:1 Cu:W reaction at a 200 °C injection temperature and isolated after 5 min (top, brown trace, 2 eq. CuBr), which the precursors ($[Ph_4P]_2WSe_4$ and CuBr (98%) in DMF) were immediately injected into the reaction vessel after sonication. The signals of Cu_2WSe_4 are weak.

With incubation of the precursors in DMF at room temperature overnight, the intensity from Cu_2WSe_4 became noticeably stronger (middle, black trace, 2 eq. CuBr (incubation)), though $[Ph_4P]CuWSe_4$ is still significant.

The isolate powders were then dried under vacuum and re-suspended in DMF with another 2 equivalences of CuBr (98%). The DMF suspension was then again injected into stirring 1-oleylamine at 200 °C for 5 min. The powders (bottom, grey trace, 2+2 eq. CuBr) were isolated after quenching from the second heating step, which contained Cu_2WSe_4 and Cu_2Se.

Cu_2Se—ICSD 41140. $[Ph_4P]CuWSe_4$ pattern was generated from published structure data.[1,2]

Figure S6

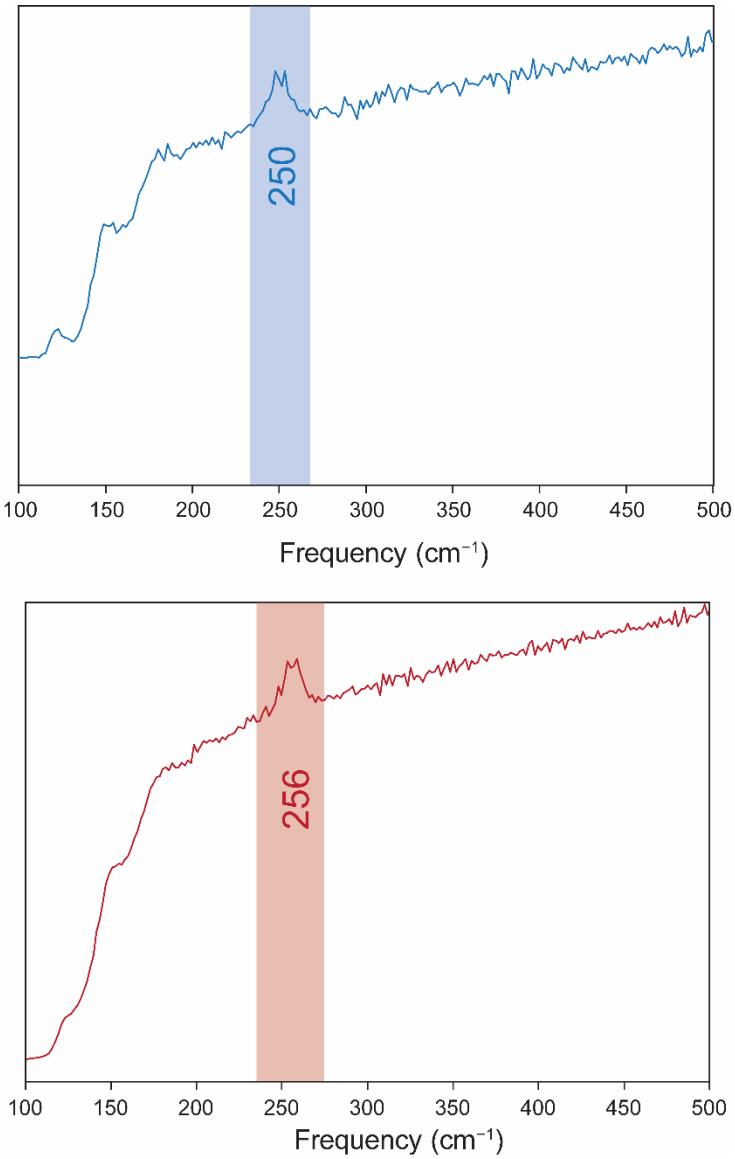

Figure S6. Raman spectra of solid pellets of Cu_2MSe_4, M = Mo/W, with characteristic M-Se vibrational mode highlighted (Mo, 250 cm^{-1}; W, 256 cm^{-1})

Theoretical Calculations

Theoretical calculations were performed using Gaussian'09 package version E.01. All structures were optimized using hybrid GGA DFT functional PBE0 (PBE1PBE keyword in Gaussian command line). The triple-zeta basis set Def2TZVP was used for all light atoms whereas Mo and W were described with SDD basis set. Structure optimization was performed in methanol environment using CPCM model of implicit solvation. All structures were true minima as was manifested by the lack of imaginary vibration frequencies in calculated IR spectra.

Table S1

Raman frequencies (in cm^{-1}) of fully symmetric 'breathing mode' vibrations of MSe_4 tetrahedra in modeled compounds. The experimental frequencies for bulk MSe_2 correspond to the combination of A1'+E' modes.

	M=Mo	M=W
MSe_4^{2-}	267	276
$Cu_2MSe_4(PH_3)_4$	275	282
$Cu_3M_2Se_8(PH_3)_4^-$	271	286
MSe_2	242[3]	251[3]

$Cu_2MSe_4(PH_3)_4$

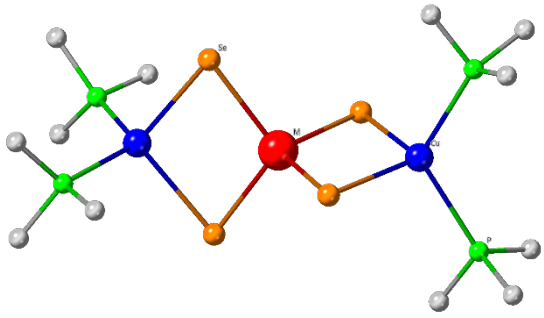

$Cu_3M_2Se_8(PH_3)_4^-$

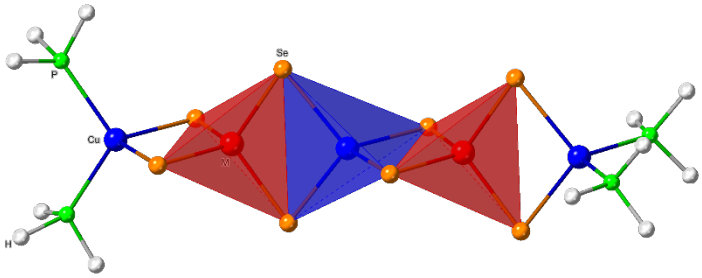

Figure S7

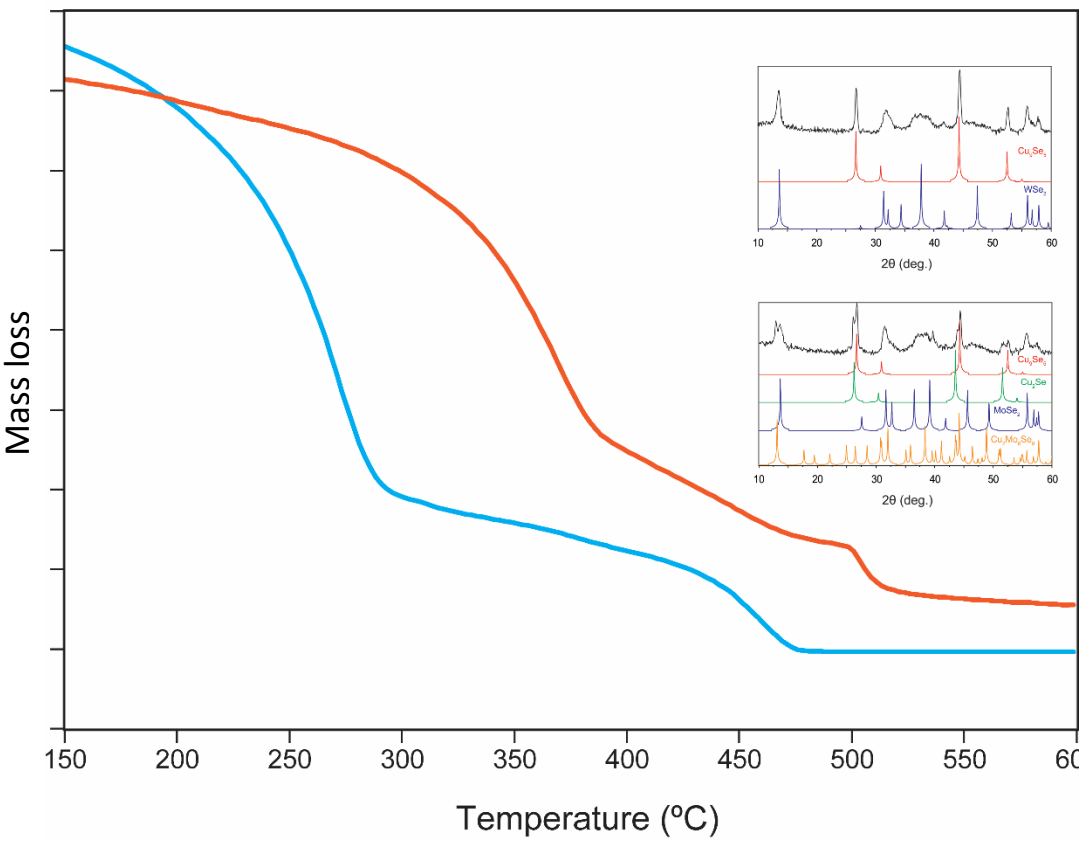

Figure S7. Thermogrativmetric curves of nanoparticles of Cu_2MoSe_4 (blue) and Cu_2WSe_4 (orange) from 150 to 600 °C, with a heating ramp of 10 °C/min under N_2 (150 mL/min). The solids after heat treatment are characterized by powder X-ray diffraction (insets). A significant portion of the mass loss before 350 °C in both systems is due to decomposition of organic ligands.

The onset of Cu_2MoSe_4 decomposition occurred at 445°C, whereas Cu_2WSe_4 started decomposing at 500ºC. The decomposition products in both cases contained MSe_2 and Cu_9Se_5. In the case of Mo, signals corresponding to Cu_2Se and $Cu_2Mo_6Se_8$ were also observed.

Cu_2Se—ICSD 41140, Cu_9Se_5—ICSD 59956, $MoSe_2$—ICSD 16948, $Cu_2Mo_6Se_8$—ICSD 628448, WSe_2—ICSD 40752

Figure S8

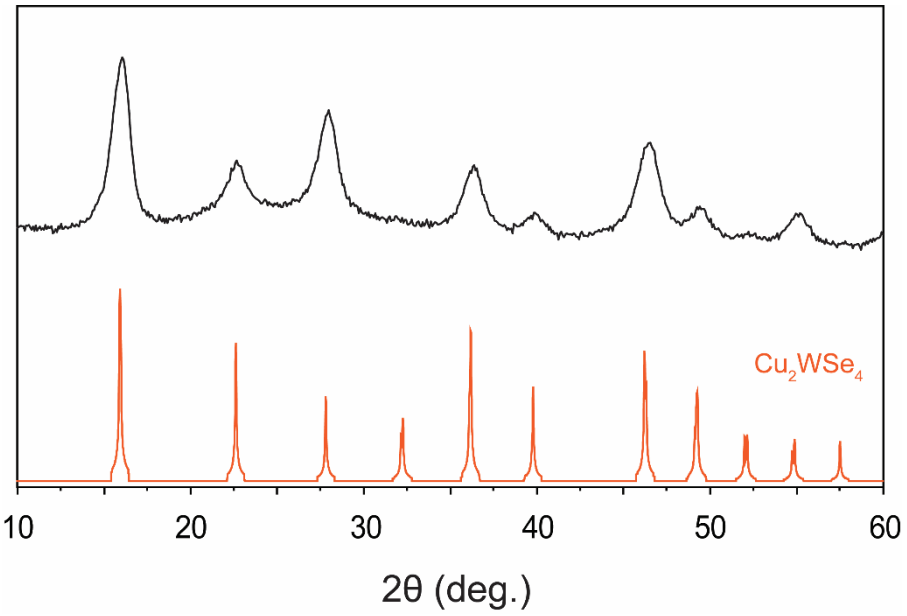

Figure S8. pXRD of a sample from a 2.4:1 Cu:W reaction between CuBr (98%) and $[Ph_4P]_2WSe_4$ at 200 °C injection temperature and isolated after 5 minutes.

Figure S9

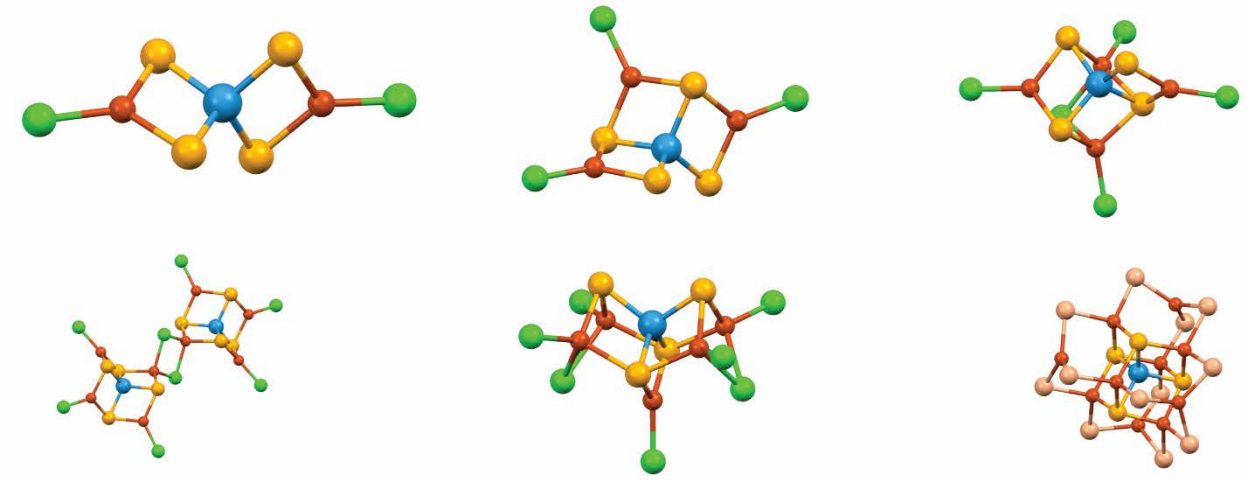

Figure S9. Various $WS_4(Cu_xCl_y)$ and $WS_4Cu_{10}Br_{12}$ fragments from crystallographic files in literature.[4–10] *W-blue, S – yellow, Cu – orange, Cl – green, Br – cherry.*

Figure S10

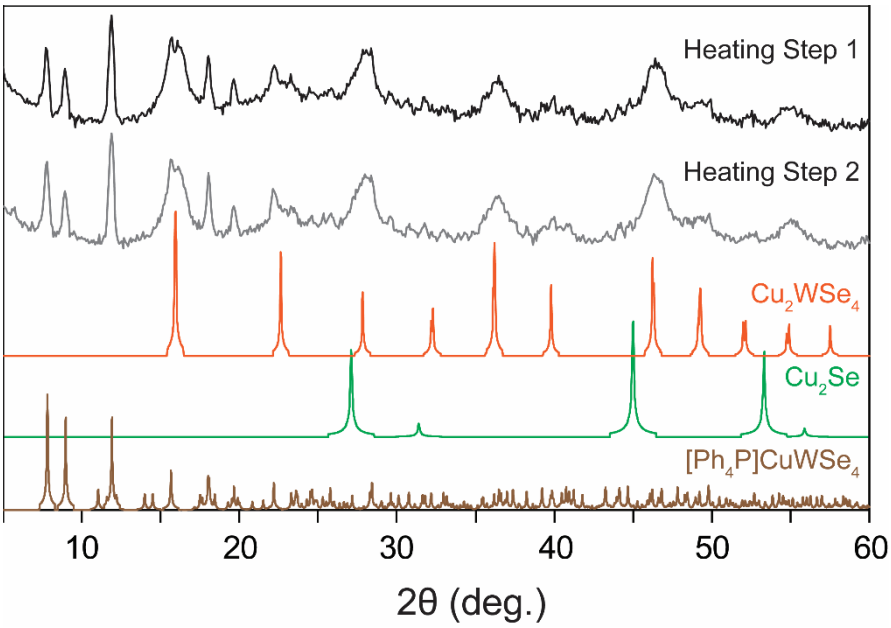

Figure S10. pXRD patterns of a sample at 200 °C injection temperature and isolated after 5 min. 2:1 Cu:W reaction (top, black trace, Heating Step 1) between CuBr (98%) and $[Ph_4P]_2WSe_4$ after incubating the precursor solutions at the room temperature overnight.

The isolate powders are then dried under vacuum and resuspended in DMF. The DMF suspension was then again injected into stirring 1-oleylamine at a 200 °C injection temperature and isolated after 5 min. The powders (bottom, grey trace, Heating Step 2) are isolated after quenching from the second heating step.

There are very little changes observed between the two experimental patterns.

Cu_2Se—ICSD 41140. $[Ph_4P]CuWSe_4$ pattern was generated from published structure data.[1,2]

Figure S11

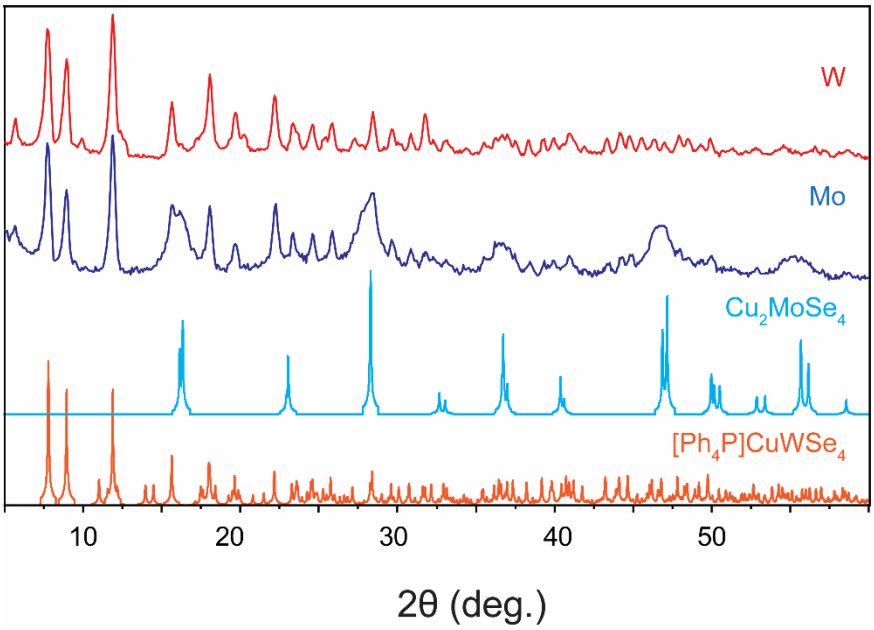

Figure S11. Experimental powder X-ray diffraction patterns of samples from 1.67:1 Cu:M (M = Mo/W) reactions between CuBr (98%) and $[Ph_4P]_2MSe_4$ at a 250 °C injection temperature and isolated after 5 minutes.

$[Ph_4P]CuWSe_4$ pattern was generated from published structure data.[1,2]

Figure S12

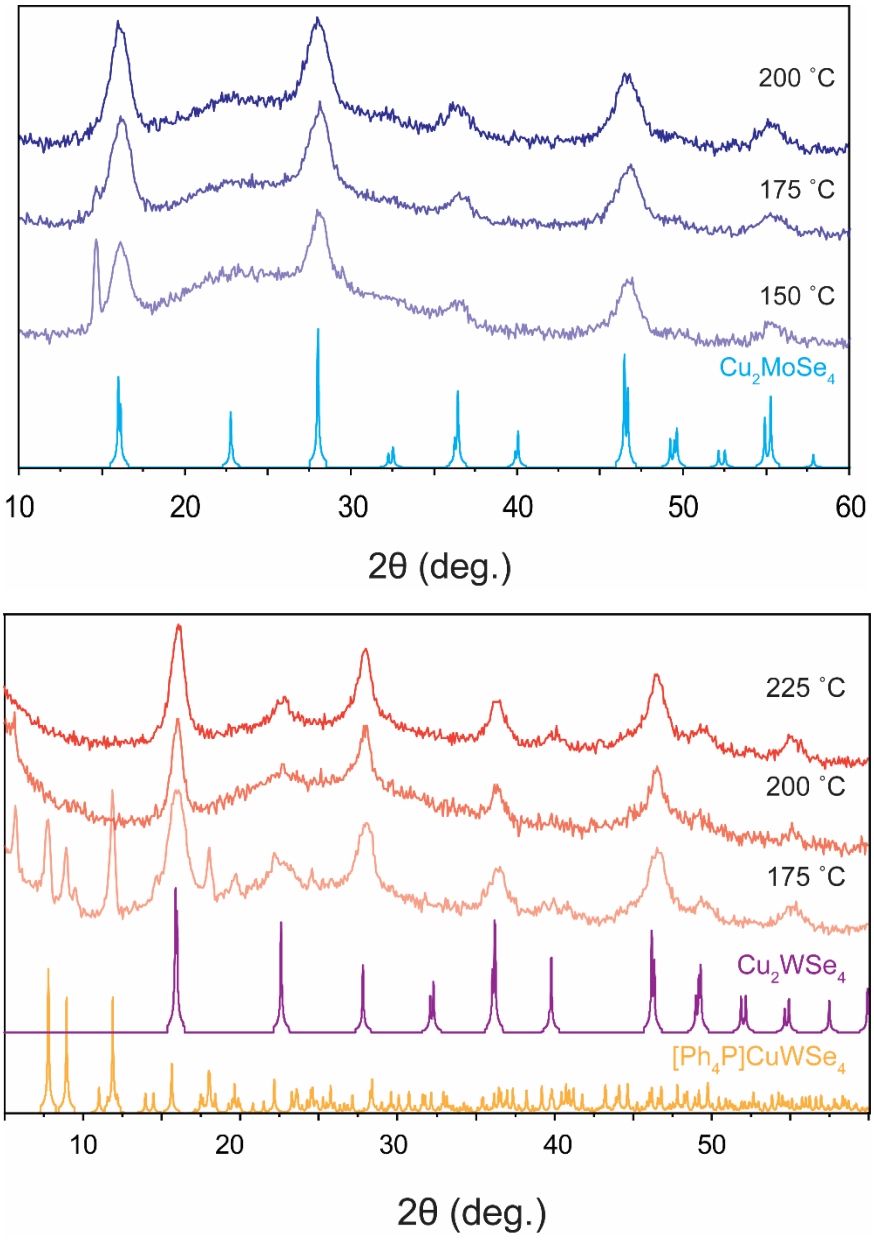

Figure S12. (Top) pXRD patterns of samples from 4:1 Cu:Mo reactions between CuBr (98%) and $[Ph_4P]_2MoSe_4$ at 150, 175, and 200 °C injection temperatures and isolated after 5 minutes. (Bottom) pXRD patterns of samples from 4:1 Cu:W reactions between CuBr (98%) and $[Ph_4P]_2WSe_4$ at 175, 200, and 225 °C injection temperatures and isolated after 5 minutes.

$[Ph_4P]CuWSe_4$ pattern was generated from published structure data.[1,2]

Figure S13

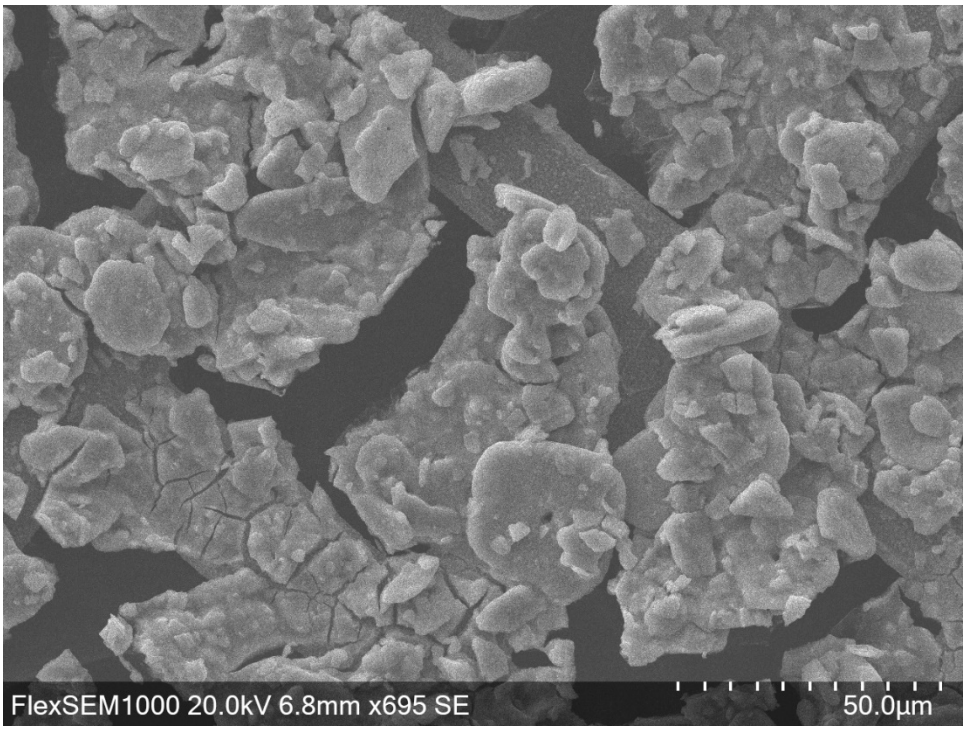

Figure S13. SEM image of larger aggregates of the ternary tetraselenomolybdates, after toluene extraction of samples synthesized from a 4:1 Cu:Mo reaction at a 200 °C injection temperature and isolated after 5 min.

Figure S14

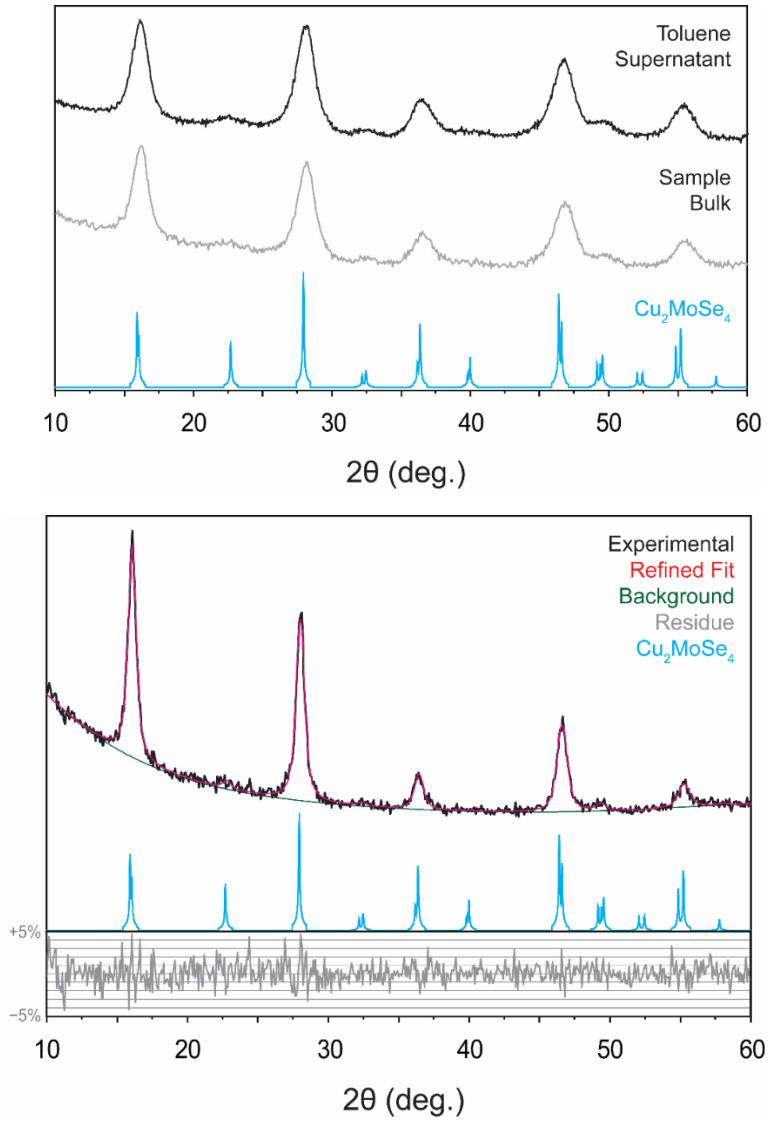

Figure S14. (Top) Powder X-ray diffraction patterns of a sample from a 4:1 Cu:Mo reaction with a 200 °C injection temperature and isolated after 5 min (middle, grey trace), and nanoparticles from toluene extraction (top, black trace). (Bottom) Results of Rietveld refinement of the toluene supernatant diffraction pattern (see conditions below).

The pXRD profile was fitted using PDXL2 software by Rigaku Inc. The fitting used Fundamental Parameter method (FP method), which decouples the profile broadening due to sample size from the instrumental broadening. Average crystallite size was found to be 16.5 nm if fit to a spherical shape. 5th degree polynomial was used to model the background and preferred orientation together with particle alignment on a substrate were taken into account with 8th degree spherical harmonics. The accounting for the preferred orientation and anisotropic alignment provides much better fit of significantly reduced intensities of 110 and 101 reflections at 22.8^{o} 2θ. Lattice parameters were refined to a=b=5.506Å, and c=5.497Å (from original a=b=5.507Å, and c= 5.553Å). Positions of Mo, Se, and Cu showed minimal changes after refinement and were fixed to their original values.

Figure S15

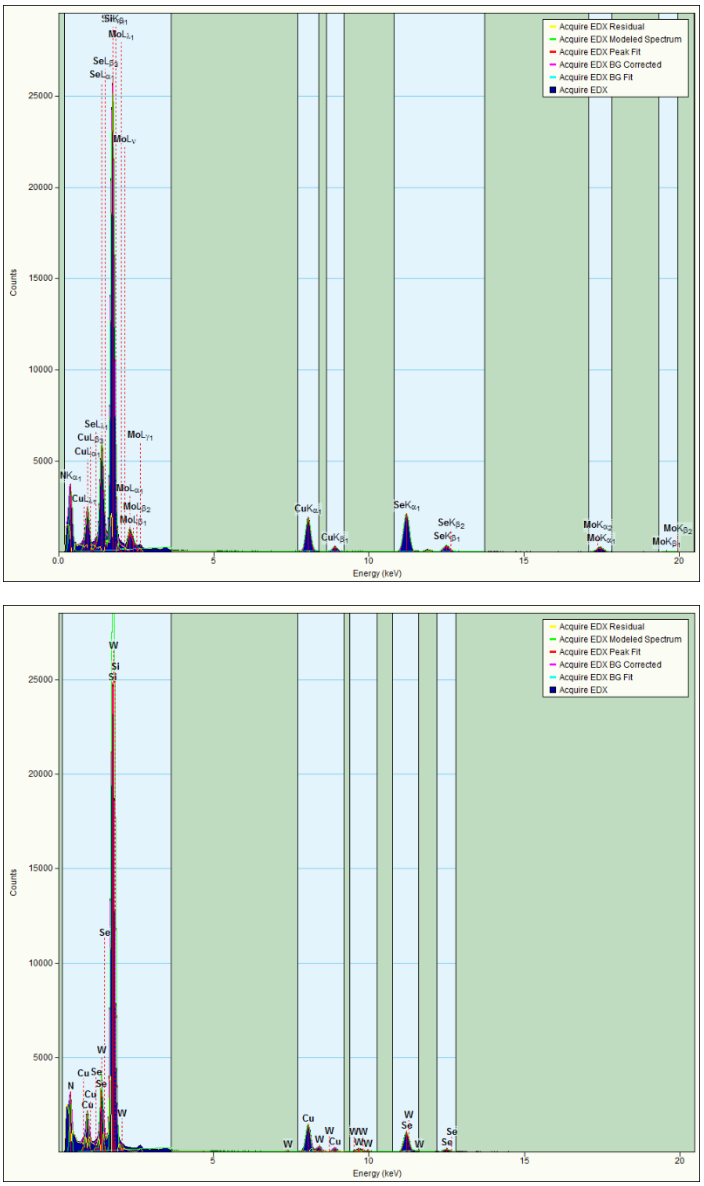

Figure S15. Energy dispersive X-ray spectra obtained from the Cu_2MoSe_4 (Cu:Mo:Se = 2.29:1:3.57) and Cu_2WSe_4 samples (Cu K and Se K interfere with W L, Cu:W:Se = 7.39:1:8.43).

Figure S16

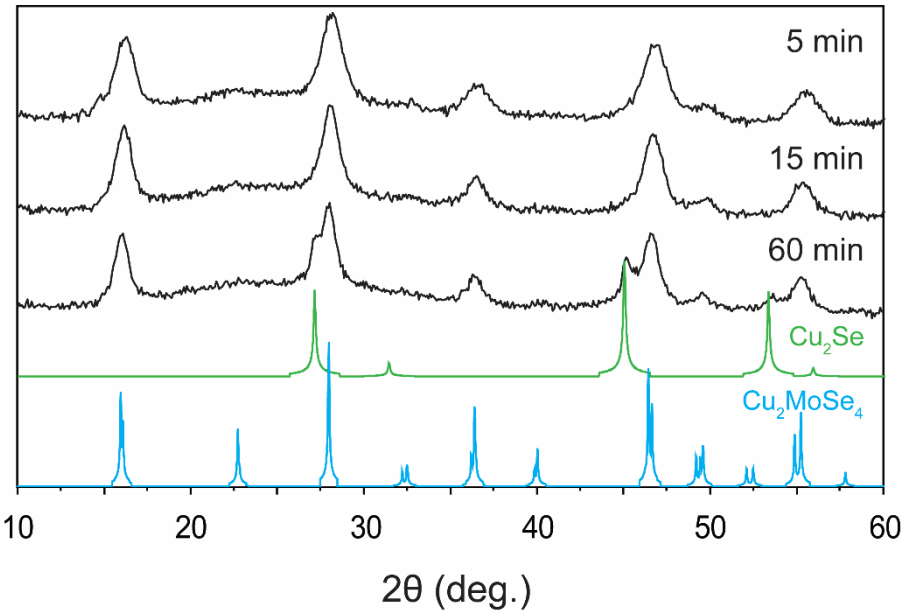

Figure S16. pXRD patterns of samples from 4:1 Cu:Mo reactions between CuBr (98%) and $[Ph_4P]_2MoSe_4$ at a 200 °C injection temperature and isolated after the set amounts of time.

Cu_2Se—ICSD 41140.

Figure S17

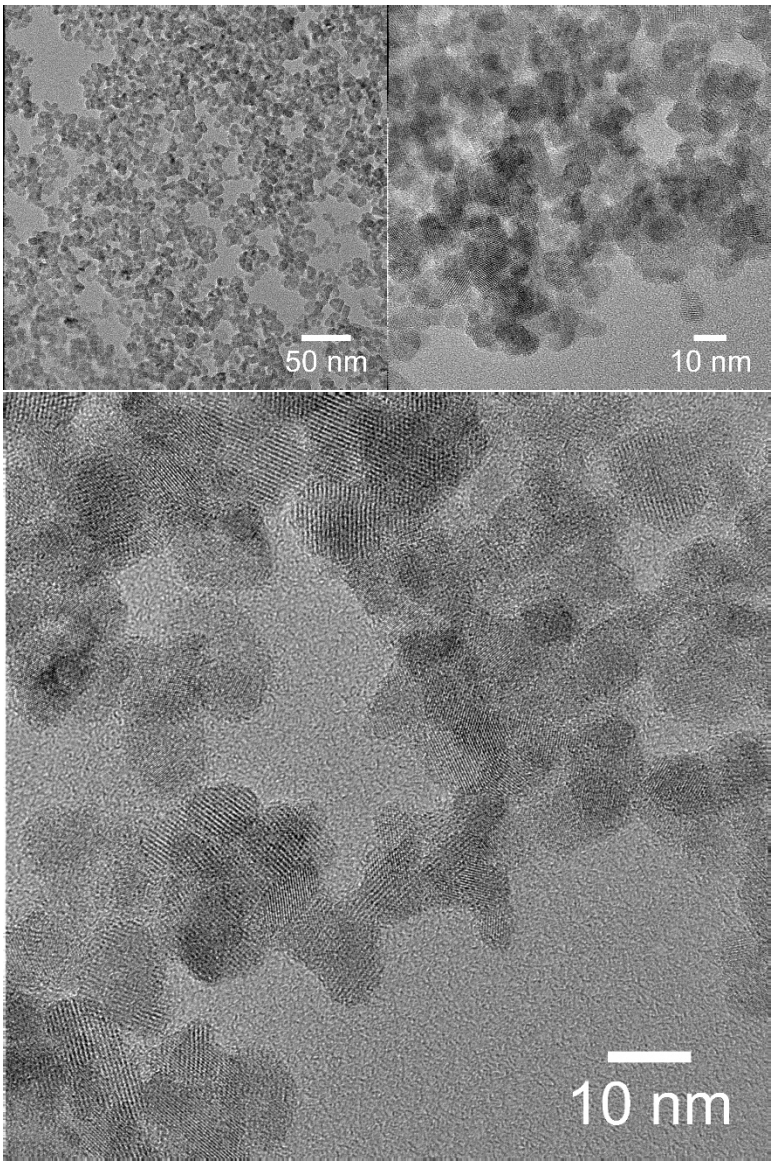

Figure S17. TEM images of a sample from a 4:1 Cu:Mo reaction between CuBr (98%) and $[Ph_4P]_2MoSe_4$ at a 200 °C injection temperature and isolated after 15 minutes.

Figure S18

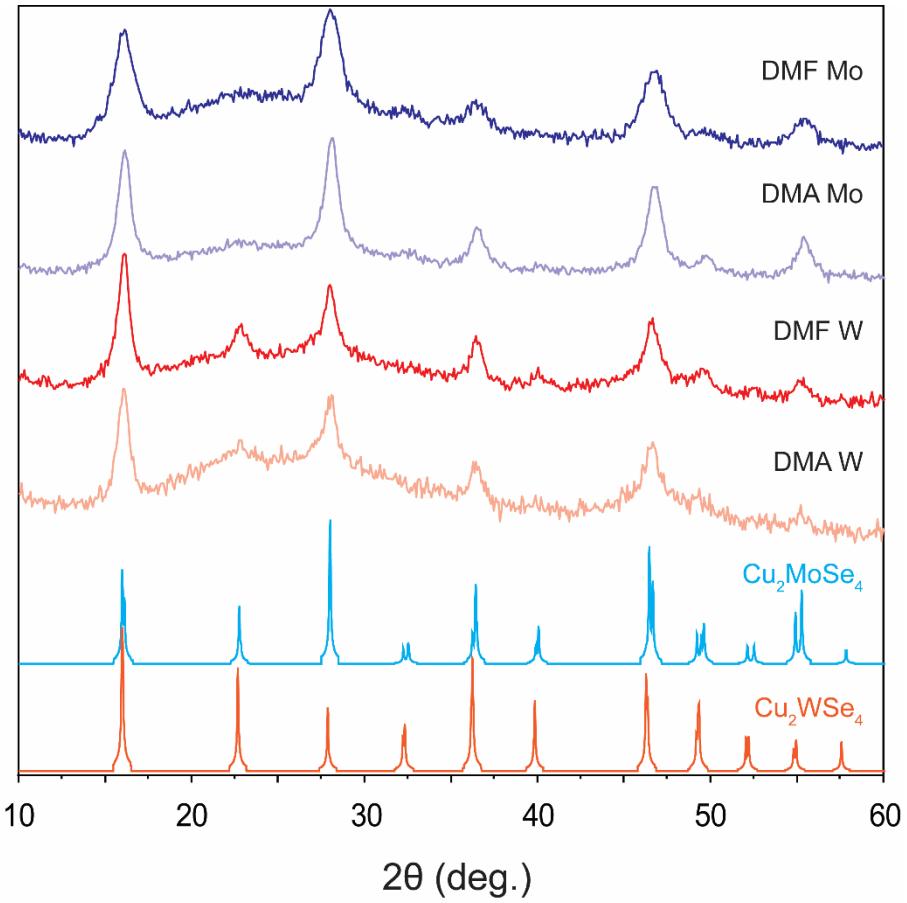

Figure S18. pXRD patterns of samples from 4:1 Cu:M reactions between CuBr (98%) and $[Ph_4P]_2MSe_4$ (M = Mo/W) at a 200 °C injection temperature and isolated after 5 minutes. The precursor carrier solvents and the nature of M are indicated at each trace.

Figure S19

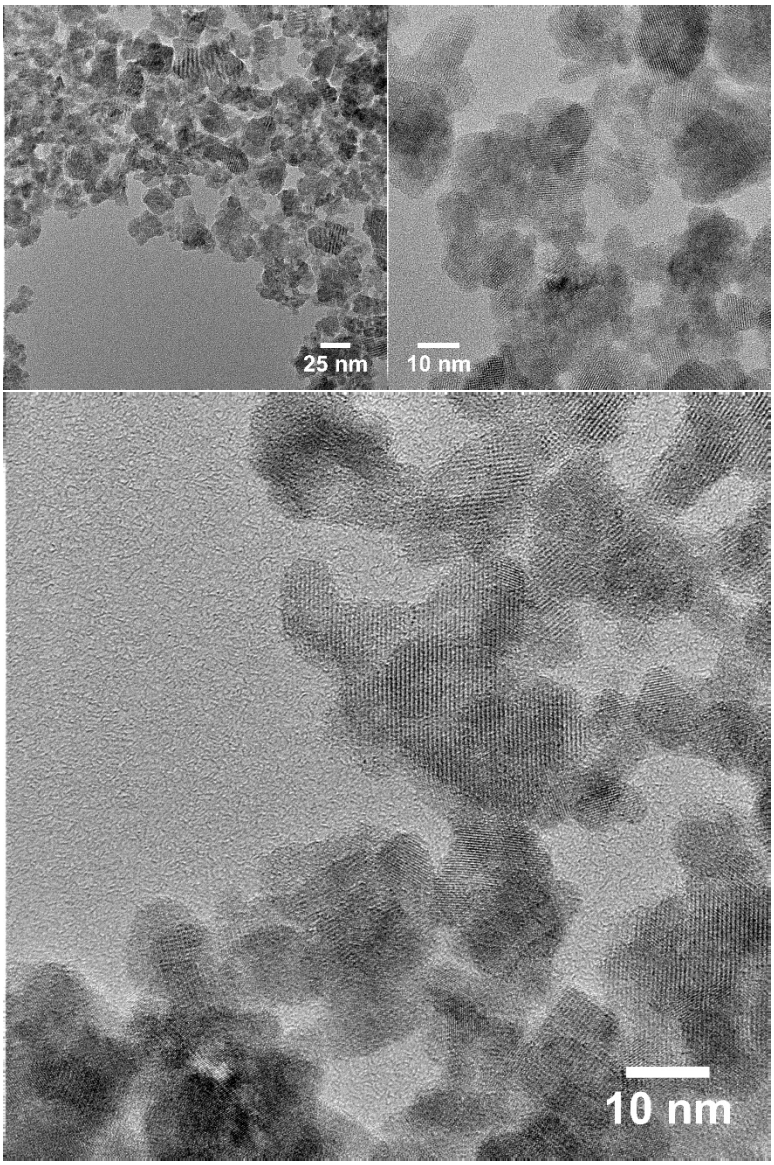

Figure S19. TEM images of a sample from a 4:1 Cu:Mo reactions between CuBr (98%) and $[Ph_4P]_2MoSe_4$ at a 200 °C injection temperature and isolated after 5 minutes. The precursor carrier solvent is DMA rather than DMF.

Figure S20

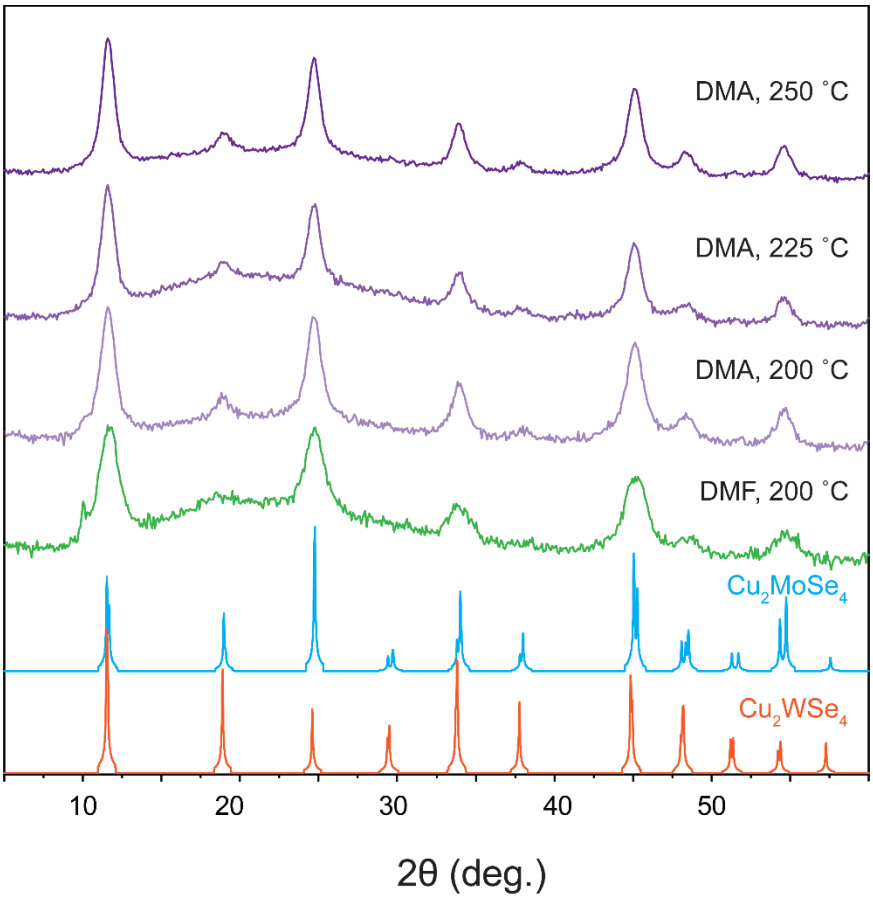

Figure S20. pXRD patterns of samples from 4:0.5:0.5 Cu:Mo:W reactions between pure CuBr and $[Ph_4P]_2MSe_4$ (M = Mo/W) at indicated injection temperatures with indicated carrier solvents, and isolated after 5 minutes. The precursor DMA solutions and DMF suspension were incubated at the room temperature overnight before injection.

Figure S21

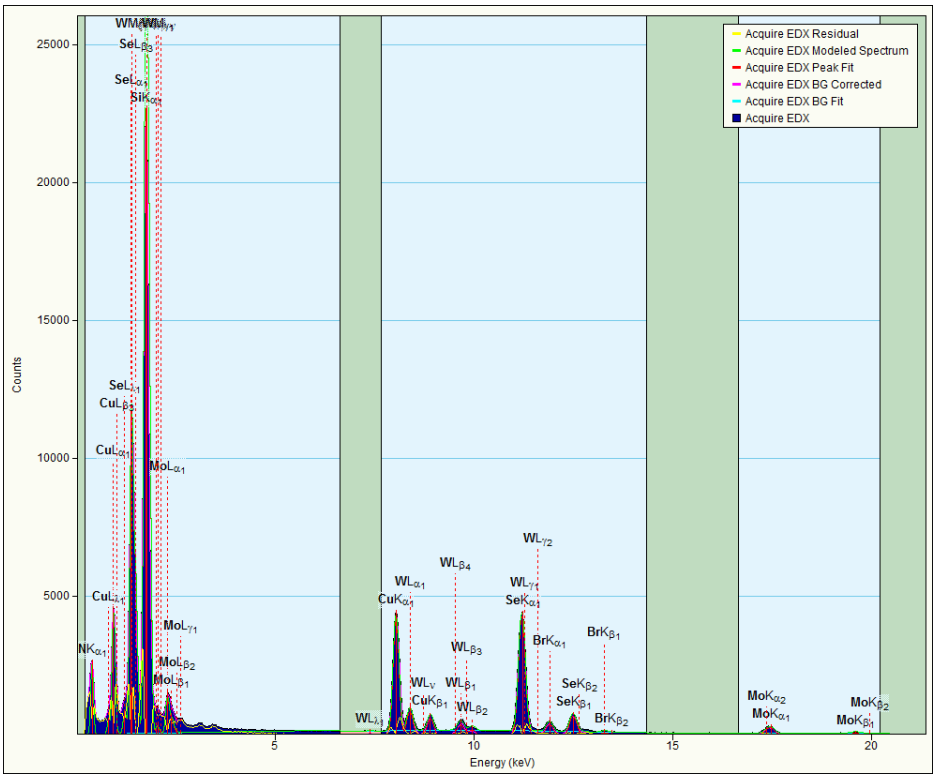

Figure S21. Energy dispersive X-ray spectra obtained from the $Cu_2Mo_{0.5}W_{0.5}Se_4$ (Cu:Mo:W:Se = 6.08:1.17:1:8.94).

Figure S22

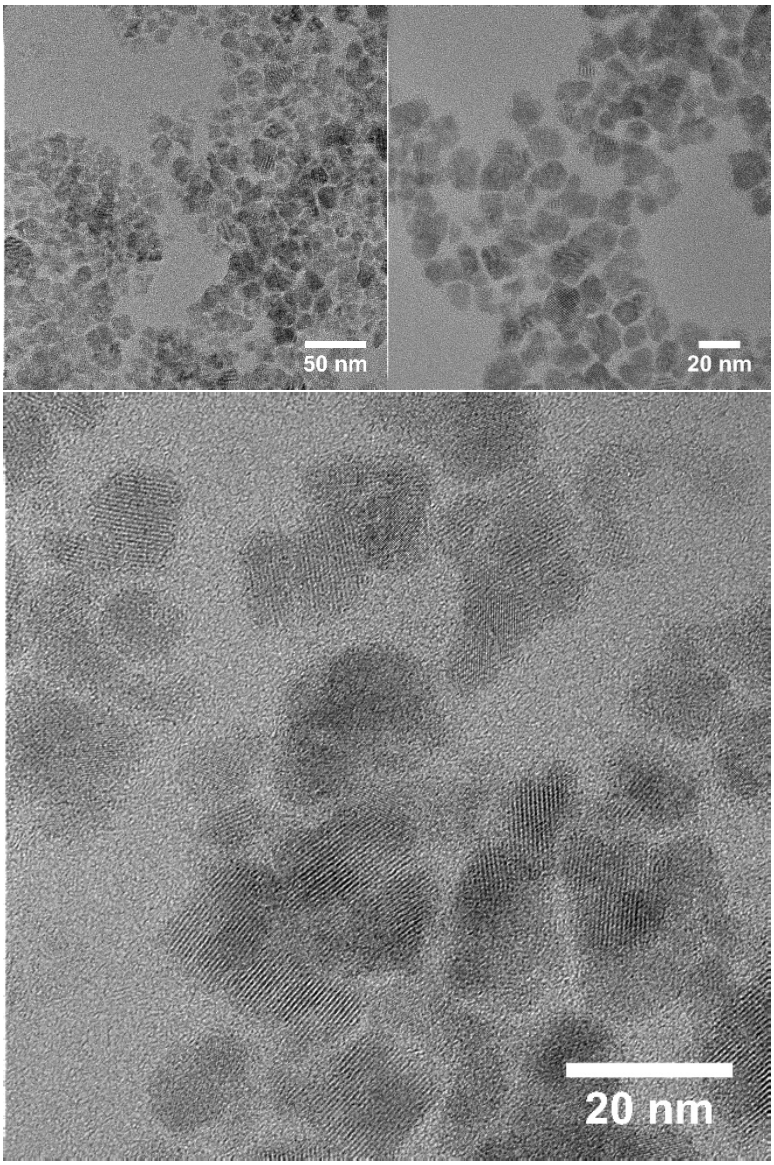

Figure S22. TEM images of a sample from 4:0.5:0.5 Cu:Mo:W reactions between CuBr (98%) and $[Ph_4P]_2MSe_4$ (M = Mo/W) at a 225 °C injection temperature and isolated after 5 minutes. The precursor carrier solvent is DMA, and the precursor solution was incubated at the room temperature overnight before injection.

Figure S23

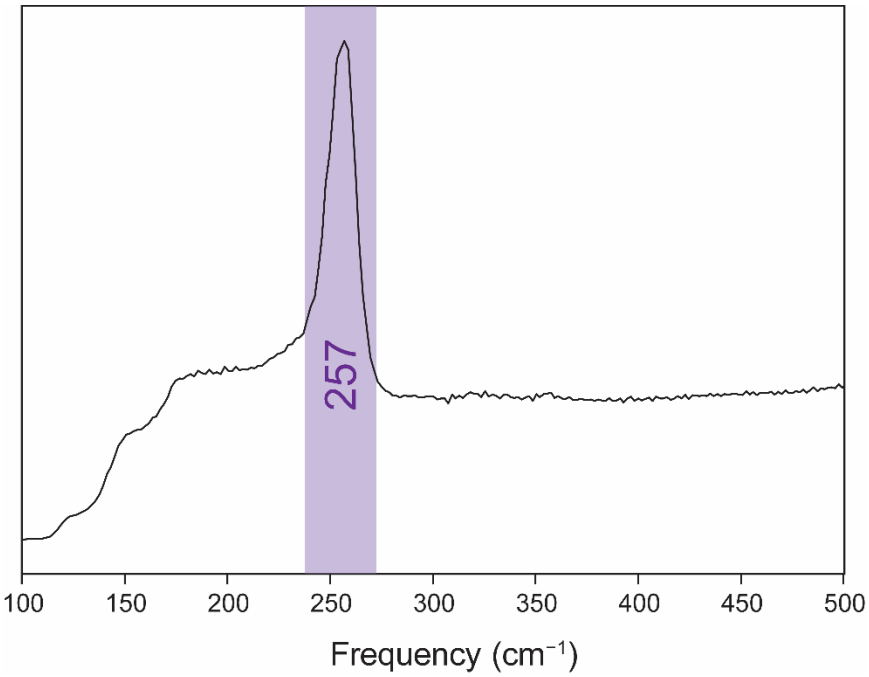

Figure S23. Raman spectrum of dropcasted film of $Cu_2Mo_{0.5}W_{0.5}Se_4$ on a glass slide, with M-Se 'breathing' vibrational mode highlighted (257 cm^{-1})

References

1 C. J. Crossland, *Solvothermal routes to new chalcogenide materials*, 2004.

2 C. J. Crossland, P. J. Hickey and J. S. O. Evans, *J. Mater. Chem.*, 2005, **15**, 3452.

3 S.-Y. Chen, C. Zheng, M. S. Fuhrer and J. Yan, *Nano Lett.*, 2015, **15**, 2526–2532.

4 J.-M. Manoli, C. Potvin and F. Secheresse, *J. Chem. Soc. Chem. Commun.*, 1982, 1159.

5 F. Sécheresse, M. Salis, C. Potvin and J. M. Manoli, *Inorg. Chim. Acta*, 1986, **114**, L19–L23.

6 W. Clegg, C. D. Scattergood and C. D. Garner, *Acta Crystallogr. Sect. C Cryst. Struct. Commun.*, 1987, **43**, 786–787.

7 F. Sécheresse, J.-M. Manoli, C. Potvin and S. Marzak, *J. Chem. Soc., Dalt. Trans.*, 1988, **5**, 3055–3057.

8 F. Sécheresse, S. Bernés, F. Robert and Y. Jeannin, *J. Chem. Soc., Dalt. Trans.*, 1991, 2875–2881.

9 Y. Jeannin, F. Sécheresse, S. Bernès and F. Robert, *Inorg. Chim. Acta*, 1992, **198**–**200**, 493–505.

10 Maochun Hong, Daxu Wu, Rong Cao, Xinjian Lei, Hanqin Liu and Jiaxi Lu, *Inorg. Chim. Acta*, 1997, **258**, 25–32.